Neural Correlates of Predictive Saccades

Stephen M. Lee[1], Alicia Peltsch[1], Maureen Kilmade[1], Donald C. Brien[1], Brian C. Coe[1], Ingrid S. Johnsrude[1,2], and Douglas P. Munoz[1]

Abstract

■ Every day we generate motor responses that are timed with external cues. This phenomenon of sensorimotor synchronization has been simplified and studied extensively using finger tapping sequences that are executed in synchrony with auditory stimuli. The predictive saccade paradigm closely resembles the finger tapping task. In this paradigm, participants follow a visual target that "steps" between two fixed locations on a visual screen at predictable ISIs. Eventually, the time from target appearance to saccade initiation (i.e., saccadic RT) becomes predictive with values nearing 0 msec. Unlike the finger tapping literature, neural control of predictive behavior described within the eye movement literature has not been well established and is inconsistent, especially between neuroimaging and patient lesion studies. To resolve these discrepancies, we used fMRI to investigate the neural correlates of predictive saccades by contrasting brain areas involved with behavior generated from the predictive saccade task with behavior generated from a reactive saccade task (saccades are generated toward targets that are unpredictably timed). We observed striking differences in neural recruitment between reactive and predictive conditions: Reactive saccades recruited oculomotor structures, as predicted, whereas predictive saccades recruited brain structures that support timing in motor responses, such as the crus I of the cerebellum, and structures commonly associated with the default mode network. Therefore, our results were more consistent with those found in the finger tapping literature. ■

INTRODUCTION

The ability to produce precisely timed motor responses is essential in many everyday tasks. This is of particular importance to musicians and dancers who must generate movements in coordination with visual or auditory cues. Studies have investigated this "sensorimotor synchronization" phenomenon using regular finger tapping to an external rhythm (see Repp, 2005, for a review). Neuroimaging studies have shown increased activation in the cerebellum during regular finger tapping to an external rhythm (Bijsterbosch et al., 2011; Lutz, Specht, Shah, & Jancke, 2000; Rao et al., 1997). The cerebellum has been well studied in its role in timing at the millisecond level (Ivry & Spencer, 2004). EEG studies have also shown involvement of other brain regions, including the primary sensorimotor, prefrontal, premotor, and posterior parietal cortices (Svoboda, Sovka, & Stancák, 2002; Gerloff et al., 1998; Knyazeva, Kurganskaya, Kurgansky, Njiokiktjien, & Vildavsky, 1994). This is supported by fMRI studies that show similar brain areas activated when processing rhythm information (Pollok, Krause, Butz, & Schnitzler, 2009; Chen, Penhune, & Zatorre, 2008; Chen, Zatorre, & Penhune, 2006; Pollok, Gross, Müller, Aschersleben, & Schnitzler, 2005; Jäncke, Loose, Lutz, Specht, & Shah, 2000). However, the neural correlates underlying this concept of predictive movement via sensorimotor synchronization have not been established for eye movement control.

A predictive saccade paradigm was developed where participants follow a visual target that alternates between fixed locations at some constant ISI (Stark, Vossius, & Young, 1962). After a few target steps, saccadic RT (SRT; the time from target appearance to saccade initiation) decreases to around 0 msec. This differs from reactive saccades, which are generated toward peripheral visual targets that appear at irregular or unpredictable times and have SRTs exceeding 100 msec (Munoz, Broughton, Goldring, & Armstrong, 1998; Fischer, Biscaldi, & Gezeck, 1997; Pierrot-Deseilligny, Rivaud, Gaymard, & Agid, 1991).

Several studies have suggested that frontal oculomotor areas are involved in generating predictive saccades (Pierrot-Deseilligny, Milea, & Müri, 2004). Behavioral deficits in the predictive saccade paradigm were observed when frontal or supplementary eye fields (FEF, SEF) or dorsolateral pFC (DLPFC) was injured or impaired (Nyffeler, Rivaud-Pechouix, Wattiez, & Gaymard, 2008; Pierrot-Deseilligny et al., 2003; Rivaud, Müri, Gaymard, Vermersch, & Pierrot-Deseilligny, 1994). However, neuroimaging studies have not been able to provide strong supporting evidence for the role of these areas in predictive saccade generation. For example, one study observed increased activation in the FEF and SEF, but not DLPFC, when comparing predictive saccades to central fixation (O'Driscoll et al., 2000), whereas another study observed increased

[1]Queen's University, Kingston, Ontario, Canada, [2]Western University, London, Ontario, Canada

© 2016 Massachusetts Institute of Technology

Journal of Cognitive Neuroscience 28:8, pp. 1210–1227
doi:10.1162/jocn_a_00968

activation in the FEF for reactive saccades when compared with predictive saccades (Simó, Krisky, & Sweeney, 2005).

Although discrepancies exist within the saccade literature, some predictive saccade studies more closely parallel the results from finger tapping studies. For instance, one finger tapping study noted a lack of activation in the DLPFC when participants tapped to a regular metronome beat (Rao et al., 1997), and another revealed increased BOLD signal in the premotor cortex, pre-SMA, and SMA when comparing irregular with regular tapping sequences (Lutz et al., 2000).

It has previously been suggested that some "internal clock" may exist in the cerebellum that drives the rhythmic-like behavior observed in predictive saccades (Joiner & Shelhamer, 2006). Of note, both increased BOLD signal (Simó et al., 2005) and increased CBF were observed in the cerebellum during predictive saccades (O'Driscoll et al., 2000). However, there is a lack of consensus about the neural control of predictive saccades because of the seemingly contradictory results between neuroimaging and lesion studies.

Here, we first conducted a behavioral experiment to optimize task conditions for eliciting predictive saccades. Then, we investigated the neural correlates of predictive saccade generation by combining the optimized behavioral task with fMRI recording to contrast the BOLD responses generated during the predictive saccade task versus a reactive saccade task. We also perform a functional connectivity analysis to characterize and contrast functional connectivity of predictive saccades and reactive saccades. Finally, we conduct a third fMRI experiment to validate our findings using a modified predictive saccade task that employs auditory stimuli instead of visual stimuli.

METHODS

All experiments were approved by the research ethics board of Queen's University (Kingston, ON), and adhered to the Canadian Tri-Council Policy Statement on Ethical Conduct for Research Involving Humans and to the Declaration of Helsinki. Written informed consent was obtained from all participants.

Experiment 1: Behavior

We first conducted a behavioral study to optimize task conditions to maximize the contrast between predictive and reactive behavior for subsequent fMRI experiments.

Participants

Twenty healthy young adults (12 women; age = 18–26 years, mean age = 20.8 years) performed the PREDICTIVE and REACTIVE saccade tasks. All participants completed a brief medical history questionnaire to ensure normal or corrected-to-normal vision, no current medications, and no history of head injury or neurological illness.

Tasks

In the PREDICTIVE task, participants were instructed to generate saccades toward a small target that alternated at a constant ISI of 500, 750, 1000, 1250, or 1500 msec between two fixed locations on the horizontal meridian (7.5° left and right of center position; Figure 1A). The REACTIVE task was similar, in that participants were required to follow the same target alternating between the same two fixed locations, but one of the five ISIs (500, 750, 1000, 1250, 1500 msec) was randomly used for each target step. Although target location was predictable, the timing of the next target appearance was unpredictable.

Data Analysis

Behavioral data were analyzed offline using custom scripts written in Matlab. Saccades were identified as changes in eye position with peak velocity exceeding 30°/sec, acceleration surpassing 9500°/sec^2, and minimum motion of the eye exceeding 0.15°. Mean SRTs were calculated for saccades within both PREDICTIVE and REACTIVE blocks. Data were excluded from a given target step if eye position data were not available because of loss of eye tracking.

Experiment 2: Behavior + fMRI

Participants

Twenty participants were separately scanned in the MRI scanner, but data from two participants were excluded from analyses because of eye tracking difficulties (e.g., obscured pupils). The remaining 18 volunteers were all right-handed (11 women) and were between 18 and 25 years (mean age = 21.3 years). All participants completed a brief medical history questionnaire to ensure normal or corrected-to-normal vision, no current medications, and no history of head injury or neurological illness.

Task and Imaging Protocol

We took advantage of the dissociation observed between predictive and reactive behavior from Experiment 1 (see Results and Figure 2A, B) and designed a task with two types of experimental blocks. The PREDICTIVE block required participants to follow a green target alternating between 10° left and right of center with a fixed ISI of 750 msec. Participants were instructed, "Move your eyes in time with the dot," as this command yielded shorter SRTs and greater proportions of predictive saccades than simply "follow the lights" (Isotalo, Lasker, & Zee, 2005). The REACTIVE block consisted of four ISIs (450, 600,

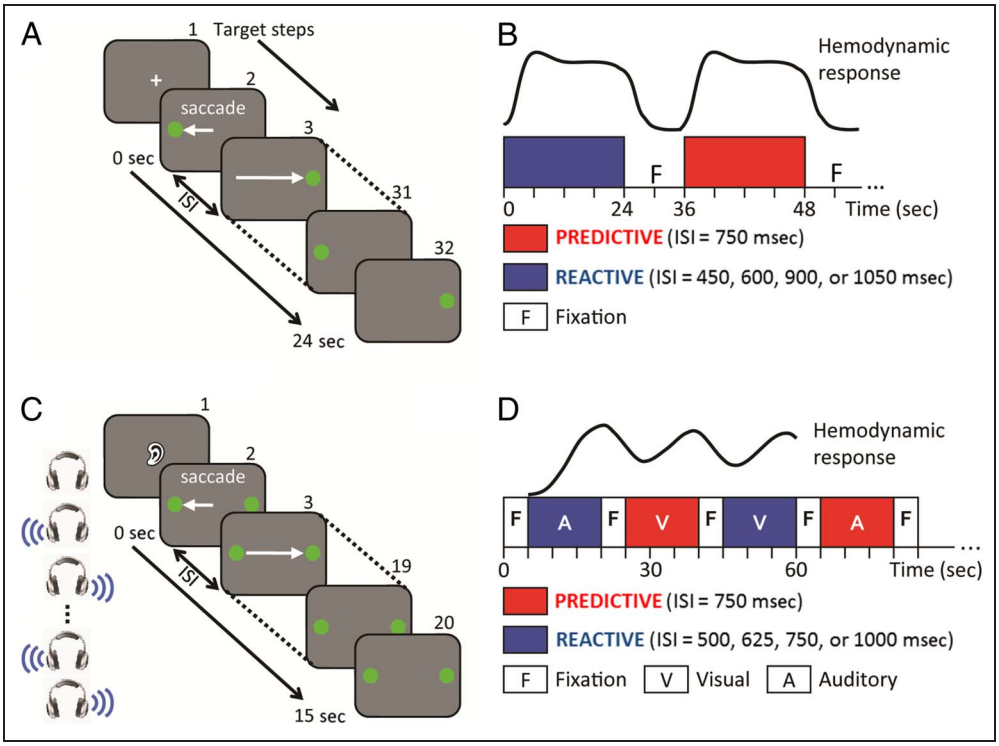

Figure 1. (A) The predictive saccade task (Experiment 2). (B) MRI protocol. Blocks were presented in alternating order. (C) The auditory saccade task (Experiment 3). (D) MRI protocol.

900, and 1050 msec) that were randomized for each target step. These were chosen to average 750 msec to help optimize imaging protocols. A control fixation block was included during which participants stared at a stationary cross at the center of the screen. Each experimental run consisted of experimental blocks presented in alternating order interleaved with control blocks (PREDICTIVE fixation–REACTIVE fixation, repeated four times; Figure 1B). All participants completed six runs. Both the PREDICTIVE and REACTIVE blocks lasted 24 sec each and were matched in terms of the number of saccades required (32 saccades per block), target eccentricity (10°), and direction (16 rightward, 16 leftward). Fixation blocks lasted 12 sec.

Participants were scanned in a Siemens 3-T whole-body MRI system (Erlangen, Germany) equipped with a head gradient set. High-resolution structural images were obtained first using a T1-weighted MPRAGE sequence, with an anterior/posterior phase-encoding direction. Functional scans consisted of T2*-weighted EPI volumes sensitive to BOLD contrast (Kwong et al., 1992; Ogawa, Lee, Kay, & Tank, 1990) acquired over six runs, each a duration of 4.8 min. Each volume consisted of 45 × 3.3 mm thick slices; flip angle = 77°; T_E = 30 msec and T_R = 3000 msec. Acquisition was transverse-oblique to avoid the eyes and to cover all of the brain, including the cerebellum. Three dummy scans were included at the beginning of each run to allow the MRI magnet to reach steady-state longitudinal magnetization.

Images were obtained using a 12-channel head coil. Participants viewed a screen via a mirror situated on top of the head coil. Visual displays were presented using custom-made software written in MatLab 7.9 (The Mathworks, Inc., Natick, MA) and projected using a NEC LT265 DLP projector. Participants were also given MR-compatible headphones to wear (NordicNeuroLab AudioSystem, Bergen, Norway). Eye movements were measured from each participant's right eye (sampling rate = 1000 Hz) using the EyeLink 1000 fiber-optic camera (SR Research, Ottawa, ON). Calibration steps were conducted at the beginning of each experimental run to ensure validity of measurements.

Data Analysis

Behavioral data were analyzed offline in the same manner as Experiment 1. Mean SRTs were calculated for the 32 target steps for both PREDICTIVE and REACTIVE blocks. Data were excluded from a given target step if eye position data were not available due to loss of eye tracking. If more than four consecutive saccades were missed, data from the entire block (24 sec) were excluded from analyses.

All fMRI data were preprocessed and analyzed using BrainVoyager (Version 1.10, Brain Innovation, Maastricht, Holland). Preprocessing steps included slice scan time correction with a cubic spline interpolation, 3-D motion correction to the first volume of each run, 3-D spatial smoothing with a 4-mm FWHM Gaussian kernel, and temporal filtering (high-pass filter with cut-off of 2 cycles/run and linear trend removal). Functional images were then coregistered to the structural image. 3-D structural images were normalized into standard Talairach space (Talairach & Tournoux, 1988). This was done by aligning them first into the AC–PC plane and then using trilinear

interpolation to warp the structural images into Talairach coordinates. These parameters were then applied to the coregistered functional data.

Our experimental tasks were modeled with boxcar predictors for the three block types used in the study: PREDICTIVE, REACTIVE, and fixation. These were convolved with BrainVoyager's 2 gamma hemodynamic response function to model the BOLD response. Additional predictors were also included for the six realignment parameters, which were covariates of no interest.

Group analysis was conducted using a random-effects general linear model. Group level statistical maps were created using a threshold of $p < .05$ and corrected for multiple comparisons (with the false discovery rate [FDR]) across the voxel population at $p < .05$ (nine contiguous voxels; estimated using BrainVoyager's Cluster Level Statistical Threshold Estimator at 1000 iterations). Brain areas showing clusters of significant activation were determined using labels corresponding to the Talairach coordinates (Talairach Daemon Client version 2.4, Research Imaging Centre, University of Texas Health Science Centre at San Antonio). Clusters of activation in the cerebellum were labeled using a 3-D MRI cerebellum atlas (Schmahmann et al., 1999). We report the peak significant voxel for all clusters in Tables 2 and 3.

We also conducted functional connectivity analyses using Granger Causality Mapping (Roebroeck, Formisano, & Goebel, 2005) to investigate the brain regions that exhibited strong correlations of activity with one another. This was assessed using the Random Effects Granger Causality Mapping v2.3 plug-in in Brain Voyager. This method required a specified brain region or seed and correlated its activity with all other voxels in the brain. For the PREDICTIVE blocks, seeds of 5 mm × 5 mm × 5 mm were selected from the peak voxels of each region found significant in the contrast between PREDICTIVE > REACTIVE. These included the medial pFC (mPFC), posterior cingulate cortex (PCC), inferior parietal lobule (IPL), and hippocampus (Figure 3 and warm colors in Figure 4). For the REACTIVE blocks, seed voxels (125 mm^3) were selected from peak voxels of cortical oculomotor areas found significant in the REACTIVE > PREDICTIVE

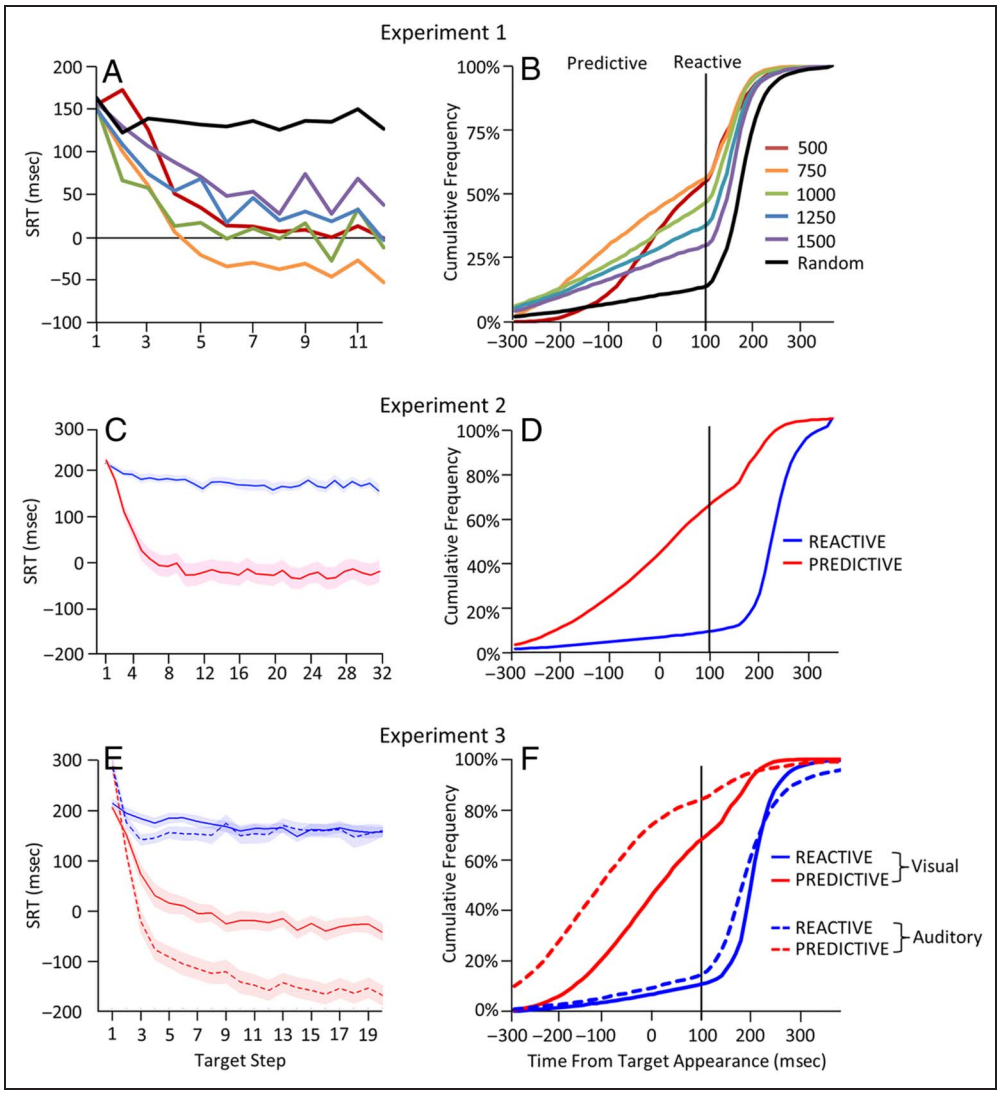

Figure 2. (A, C, E) Mean SRT plots for each target step (different colors depict each ISI). (B, D, F) Cumulative distribution of SRTs by experimental condition (blue, reactive; red, predictive).

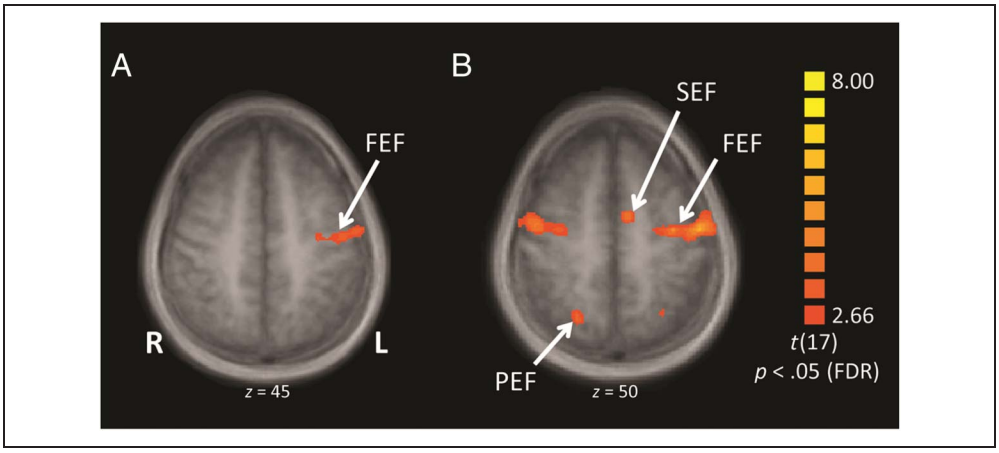

Figure 3. Experiment 2. Contrast maps comparing saccade tasks (Predictive, Reactive) to fixation. (A) Predictive > Fixation. (B) Reactive > Fixation.

contrast. These were the FEF, SEF, parietal eye field (PEF), and DLPFC. Using these seeds, we first assessed functional connectivity at the single-subject level: Instantaneous correlations were calculated for BOLD activation produced during the PREDICTIVE and REACTIVE tasks. The resulting statistical maps for each participant were included in group level analyses, where we performed a group t test comparing all voxels to a baseline of zero.

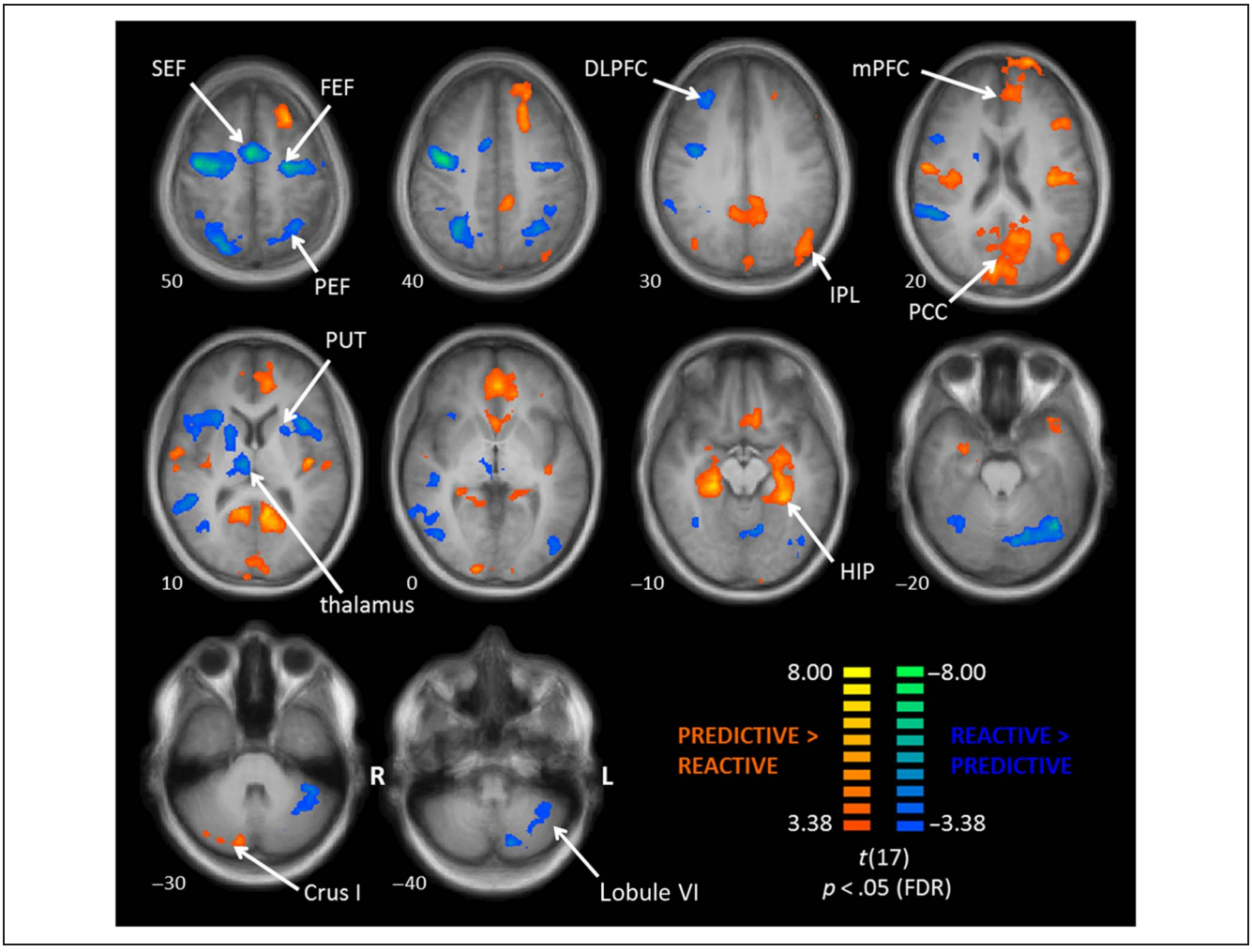

Figure 4. Experiment 2. Contrast map showing REACTIVE subtracted from PREDICTIVE. Voxels that yield positive values (PREDICTIVE > REACTIVE) are shown in orange/yellow, and those that yield negative values (REACTIVE > PREDICTIVE) are shown in blue/green. Images were thresholded at $p < .05$ (FDR-corrected) and at cluster sizes of at least 9 voxels. Coordinates are in the Talairach z plane.

Experiment 3: Behavior + fMRI

We recognized that visual stimulation differed between the two tasks in Experiment 2 because, in the REACTIVE task, the unpredictable target appeared in the peripheral retina, but in the PREDICTIVE task, participants continuously foveated the visual stimuli once SRTs settled near 0 msec. To control for these differences in visual stimulation, we modified the task using auditory stimuli to elicit predictive and reactive behavior while holding visual stimulation constant.

Participants

Nineteen right-handed volunteers (10 women) were recruited for this experiment and were between 19 and 29 years (mean age = 22.4 years). Data from only one participant were excluded from analysis due to eye tracking difficulties. All participants completed a brief medical history questionnaire to ensure normal or corrected-to-normal vision, no current medications, and no history of head injury or neurological illness.

Task and Imaging Protocol

Participants performed four saccade tasks in the MRI scanner: two visual (PREDICTIVE/REACTIVE) and two auditory (PREDICTIVE/REACTIVE). The visual PREDICTIVE task was the same as described in Experiments 1 and 2 with a fixed 750-msec ISI (Figure 1A). In the visual REACTIVE task, we used five ISIs that were randomized for each target step (500, 625, 750, 875, 1000 msec). Five ISIs were used because block durations were shortened, and each ISI was presented with equal frequency. Both visual tasks were 15 sec long (20 target steps) and were matched in terms of the number saccades (20 saccades per block), target amplitude (10°), and direction (10 right, 10 left).

In the two tasks that employed auditory cues, short white noise bursts of 100-msec duration were used. Participants were instructed to generate saccades toward the direction of the sound, and the timing was either regular (PREDICTIVE) or randomized (REACTIVE; Figure 1C), using the same ISIs described above. The visual display shown during the auditory tasks consisted of two targets that remained fixed on the screen at 10° left and right of center throughout the duration of a block. Participants listened for the noise burst presented to the left or right ear via headphones and subsequently generated a saccade toward the corresponding visual target. Both auditory tasks were 15 sec in duration (20 target sounds) and were matched in terms of the number of saccades required (20 saccades per block), target amplitude (10°), and direction (10 right; 10 left).

Blocks of fixation were interleaved between experimental blocks and were varied at 3, 5, or 7 sec. This jittering of duration was done intentionally to avoid biasing effects that may result from having regular events at integer durations of the acquisition time (T_R) for the PREDICTIVE tasks (Amaro & Barker, 2006). Fixation cues consisted of small pictorial images that guided participants to what task would be presented next (i.e., ear = auditory, eye = visual). The image color indicated if the ISI would be constant (white) or random (red).

All participants completed five runs. Each run consisted of the four experimental conditions (visual: PREDICTIVE, REACTIVE; auditory: PREDICTIVE, REACTIVE) presented in 15-sec blocks that were interleaved with periods of fixation (Figure 1D). Within a run, these four different block types were presented four times each. The block order was pseudorandomized and counterbalanced across the five runs.

MRI procedure was largely the same as in Experiment 2. Functional scans consisted of T2*-weighted EPI volumes that were acquired over five runs, each approximately 5 min. Two dummy scans were included to allow the MRI magnet to reach steady state longitudinal magnetization. Each volume consisted of 41 × 3.3 mm thick slices; flip angle = 83°; T_E = 30 msec and T_R = 2750 msec.

Data Analysis

In addition to SRTs, we also calculated saccade metrics, including amplitude, duration, and peak velocity for saccades with SRTs <100 msec in the PREDICTIVE blocks and for saccades with SRTs >100 msec in the REACTIVE blocks (Figure 3). This was done to confirm that participants not only received similar visual stimulation between PREDICTIVE and REACTIVE auditory tasks but that they also produced similar saccade metrics. Saccade amplitude was measured as the distance (in degrees) between the start and end points of the saccade, and accuracy was measured as the distance (in degrees) from the final end point of the saccade to the location of the visual target.

All fMRI data were preprocessed and analyzed as described in Experiment 2 but using five boxcar predictors: PREDICTIVE (visual, auditory), REACTIVE (visual, auditory), and fixation. Criterion for reporting and labeling peak voxels also remained the same (see Table 3 and Table 4).

RESULTS

Experiment 1

The results from the first behavioral experiment revealed that an ISI of 750 msec yielded saccades with the shortest SRTs and the greatest percentage of predictive saccades (orange curves in Figure 2A, B). Therefore, we used this ISI for the predictive tasks in fMRI Experiments 2 and 3. The dissociation between random ISIs and fixed ISIs is obvious in Figure 2A (contrast black and orange curves). Furthermore, the cumulative RT distributions in Figure 2B revealed a sharp increase in the number of

saccades with SRTs over just 100 msec, regardless of ISI. This value marked the time at which visual target information influenced saccade production (Munoz et al., 1998; Pettsch, Hemraj, Garcia, & Munoz, 2011). Any saccade generated with an SRT <100 msec was not likely influenced by visual target appearance and was classified as predictive. Therefore, in the remaining two experiments, we defined "predictive saccades" as those saccades having SRTs <100 msec and "reactive saccades" as those having SRTs >100 msec. This criterion was used in all subsequent analyses.

Experiment 2

Behavior

Participants exhibited clear predictive behavior in the scanner. Figure 2C shows the mean SRTs for every target step for both the PREDICTIVE (red) and REACTIVE (blue) tasks, and Figure 2D illustrates the cumulative distributions of SRTs. As expected, the cumulative distributions for the PREDICTIVE and REACTIVE blocks were significantly different ($p < .001$, Kolmogorov–Smirnov test), demonstrating that a greater proportion of predictive saccades were generated in the PREDICTIVE task compared with the REACTIVE task.

Similar to Experiment 1, the REACTIVE task elicited almost exclusively reactive saccades for all target steps (SRTs >100 msec). In the PREDICTIVE task, saccades reached predictive levels (SRT <100 msec) by Target Step 3 and appeared to plateau by about Target Step 7 at a value near 0 msec (Figure 2C). Paired-samples t tests were conducted to compare the 32 target steps between the two saccade tasks (Bonferroni-corrected). Apart from the first target step ($t(17) = 1.70$, $p = .11$), SRTs for all target steps in the REACTIVE task were significantly greater than the corresponding steps in the PREDICTIVE task ($ps < .001$). Thus, participants were appropriately generating reactive saccades in the REACTIVE task and predictive saccades in the PREDICTIVE task.

Imaging

We conducted two contrasts comparing both PREDICTIVE and REACTIVE tasks with fixation (Figure 3). Clusters of significant activation are displayed in Table 1. For REACTIVE > fixation, we found increased activation in SEF and bilateral FEF and PEF. For PREDICTIVE > fixation, there was a lack of activation in these areas except for left FEF.

We then conducted two additional contrasts of interest and their main peaks of activation clusters are displayed in Table 2. The PREDICTIVE > REACTIVE contrast (warm colors) revealed increased activation in areas including

Table 1. Experiment 2: MRI Activation Peaks for Saccade Tasks (PREDICTIVE, REACTIVE) Compared with Fixation

	Talairach Coordinates				
Anatomical Region	*x*	*y*	*z*	*t*	*Size (Voxels)*
PREDICTIVE > Fixation					
L lingual gyrus	0	−76	−2	11.25	1750
L FEF	−45	−10	43	4.55	75
L MOG	−42	−73	4	4.22	35
REACTIVE > Fixation					
L lingual gyrus	−6	−82	−5	10.86	1506
L FEF	−45	−10	43	8.42	200
R FEF	42	−7	46	6.12	135
SEF	−6	−7	55	6.79	109
L putamen	−21	−7	10	5.27	52
R putamen	18	5	7	5.96	56
L MOG	−42	−73	4	5.09	77
L PEF	−27	−49	43	3096	27
R PEF	21	−58	49	4.57	21
R MTG	36	−64	7	4.05	45

x, *y*, *z* Talairach coordinates specify the location of the peak voxel (highest *t* value) of a cluster in an anatomical region. L = left, R = right; MOG, middle occipital gyrus; MTG, middle temporal gyrus.

Table 2. Experiment 2: MRI Activation Peaks for PREDICTIVE–REACTIVE

	Talairach Coordinates				
Anatomical Region	*x*	*y*	*z*	*t*	*Size (Voxels)*
PREDICTIVE > REACTIVE					
L insula (posterior)	−39	−16	13	8.19	161
R insula (posterior)	36	−13	16	6.17	92
R precentral gyrus	57	−10	13	7.70	168
mPFC/ACC	−3	41	1	7.30	497
L SFG	−24	23	49	6.50	170
L MFG	−39	23	19	5.04	47
L PCC	−9	−49	7	8.37	398
L PCC	−9	−40	34	7.41	127
R PCC	15	−55	16	6.27	138
L IPL	−42	−73	25	6.35	170
R precuneus	9	−49	31	5.04	25
L parahippocampal gyrus	−30	−37	−8	8.02	203
R parahippocampal gyrus	24	−28	−11	8.00	203
R cuneus	3	−79	22	7.37	219
R lingual gyrus	12	−91	1	5.99	24
R cerebellum (crus I)	12	−76	−32	5.89	73
REACTIVE > PREDICTIVE					
L FEF	−24	−10	49	6.95	180
R FEF	39	−4	43	9.32	489
L insula (anterior)	−33	11	16	6.30	84
R insula (anterior)	27	17	13	5.63	184
R DLPFC	27	41	37	5.06	54
L PEF	−30	−52	46	6.48	181
R PEF	30	−58	37	6.40	302
R STS and R angular gyrus	42	−25	−2	5.75	246
L IOG	−42	−76	−5	7.81	72
R MOG	36	−64	4	5.84	104
L cerebellum (lobule VI)	−39	−58	−20	6.73	420
R thalamus	15	−19	13	6.37	117
L putamen	−21	11	7	4.75	17
R putamen	27	17	13	5.63	257

x, *y*, *z* Talairach coordinates specify the location of the peak voxel (highest *t* value) of a cluster in an anatomical region. L = left, R = right; SFG/MFG, superior and middle frontal gyrus; MOG/IOG, middle and inferior occipital gyrus.

the PCC, mPFC, bilateral hippocampus, bilateral IPL, and right cerebellum (crus I; Figure 4). On the other hand, the REACTIVE > PREDICTIVE contrast (cool colors) showed greater activation in oculomotor areas including the key cortical eye fields (i.e., FEF, SEF, PEF) and right DLPFC, as well as the cerebellum (lobule VI; Figure 4).

Lastly, we conducted functional connectivity analyses using Granger Causality, and results are displayed in

Figure 5. Areas in orange reflect statistically significant correlations that survived a threshold t value of 4.52 ($p < .0003$, uncorrected) and were larger than 10 voxels. For the PREDICTIVE blocks (Figure 5A), activity in all seed ROIs (hippocampus, IPL, mPFC, PCC) was significantly correlated with each other. Similarly, all seeds for the REACTIVE blocks (DLPFC, FEF, PEF, SEF; Figure 5B) were significantly correlated to one another. This supports the idea that two dissociated neural networks may be controlling behavior in the PREDICTIVE task versus the REACTIVE task.

Experiment 3

Behavior

The auditory stimuli produced similar predictive and reactive saccade behavior as visual stimuli. Figure 2E displays the averaged SRTs for all four saccade tasks and again clearly dissociates predictive and reactive behavior for both visual and auditory conditions. Both REACTIVE tasks elicited reactive saccades (most SRTs >100 msec) from Target Steps 1 to 20. However, in the PREDICTIVE tasks, average SRTs fell below 100 msec by Target Step 3. Interestingly, SRTs in the visual PREDICTIVE task fell below zero to plateau at around −30 msec, whereas in the auditory PREDICTIVE task, SRT values reached a much earlier value of approximately −150 msec. This is consistent with previous finger tapping studies that have shown that auditory tasks appear to generate faster RTs than visual tasks (Pollok et al., 2009; Jäncke et al., 2000; Penhune, Zatorre, & Evans, 1998; Kolers & Brewster, 1985). SRTs reaching negative values in both visual and auditory PREDICTIVE tasks indicate that participants on average initiated the saccade before the next target was either seen or heard.

Kolmogorov–Smirnov tests were conducted to determine differences between the cumulative distributions of SRTs between conditions. Figure 2F shows that the PREDICTIVE task elicited a significantly greater percentage of predictive saccades than the REACTIVE task in both the visual ($p < .001$) and auditory conditions ($p < .001$). There was no significant difference between the two PREDICTIVE tasks ($p = .34$) or the two REACTIVE tasks ($p = .08$). This shows that similar predictive or reactive saccade behavior was elicited with both visual and auditory cues.

We also analyzed saccade metrics to confirm they did not change. A 2 × 2 repeated-measures ANOVA was conducted for all three saccade measures (i.e., amplitude, accuracy, peak velocity). The variables were Task (PREDICTIVE, REACTIVE) and Modality (visual, auditory). For saccadic amplitude (Figure 6A), we found a significant main effect of Modality ($F(1, 17) = 23.21, p < .001$) but no significant main effect of Task ($F(1, 17) = .32, p = .58$) or interaction effect ($F(1, 17) = 2.06, p = .17$). The visual tasks showed a tendency to undershoot the full 20° amplitude between target locations compared with the auditory tasks. This is likely because of the fact that fixed placeholders were used in auditory tasks whereas a transient jumping target was used in the visual tasks.

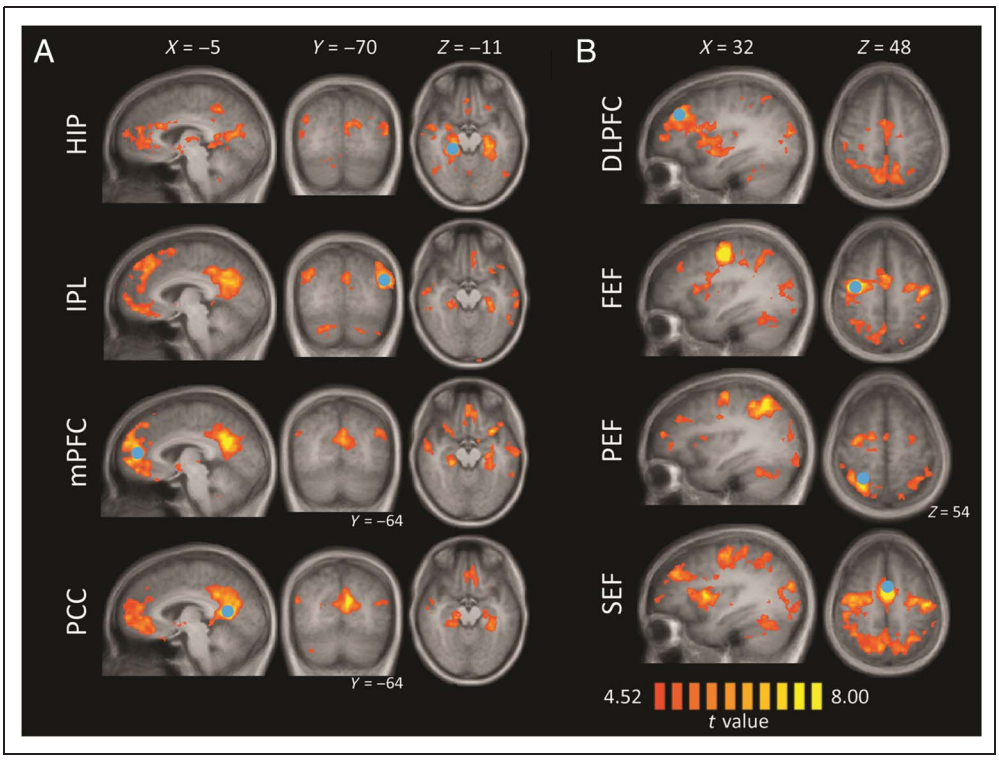

Figure 5. Experiment 2. Functional connectivity map displaying areas having correlated activity with seed regions for (A) the predictive saccade task and (B) the reactive saccade task. Images are thresholded at $p < .0003$ (uncorrected). Seeds are indicated with blue circles.

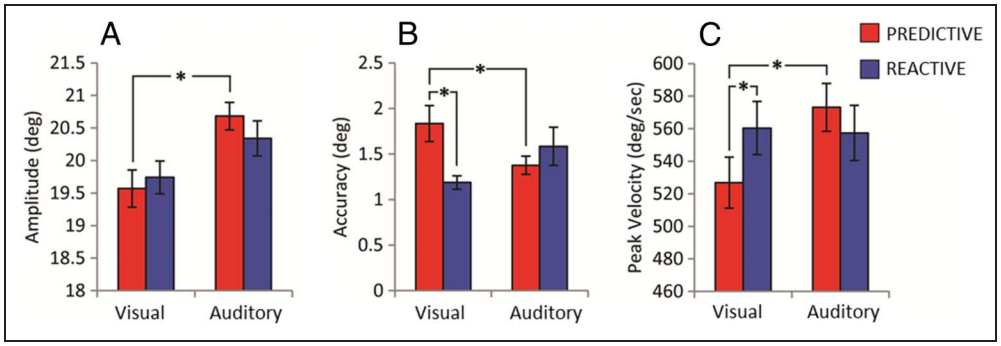

Figure 6. Saccade metrics from Experiment 3: (A) amplitude, (B) accuracy, and (C) peak velocity. Asterisks denote significant differences (p = .01) in saccade metrics between tasks (predictive vs. reactive), or modalities (visual vs. auditory)

For saccade accuracy (Figure 6B), there was no significant main effect of Modality ($F(1, 17) = .05$, $p = .83$) or Task ($F(1, 17) = 2.78$, $p = .11$), but a significant interaction effect was observed ($F(1, 17) = 14.80$, $p < .01$). To follow up the interaction effect, we conducted pairwise comparisons (Sidak-corrected), which revealed that saccades from the visual PREDICTIVE task showed the greatest deviation from target compared with both visual REACTIVE ($p < .01$) and auditory REACTIVE ($p < .01$) tasks. This was not unexpected because, in the REACTIVE tasks, the next target appeared just before a saccade was generated, whereas in the visual PREDICTIVE task, saccades were largely generated before the target appeared (SRTs ≤ 0 msec) and were not visually triggered and therefore less accurate.

Lastly, for peak velocities (Figure 6C), we found both a significant main effect of Modality ($F(1, 17) = 19.19$, $p < .001$) and a significant interaction effect ($F(1, 17) = 26.06$, $p < .001$). No main effect of Task was noted ($F(1, 17) = .65$, $p = .43$). Pairwise comparisons (Sidak-corrected) revealed that saccades in the visual PREDICTIVE task were significantly slower than visual REACTIVE ($p < .05$) and auditory PREDICTIVE ($p < .001$) tasks. Again, visual information about the subsequent target was not present for the visual PREDICTIVE task when SRTs reached below 0 msec, compared with the other three tasks.

In summary, our saccade metric data reveal that behavior in the visual PREDICTIVE task is most distinct from all other tasks, as expected. Saccades were slower and less accurate because they were not directed to visual stimuli. We were also able to confirm that there was no significant difference in behavior between our auditory PREDICTIVE and REACTIVE tasks as measured by saccade amplitude, accuracy, and peak velocity. Therefore, differences in neural processing observed in our fMRI data between the auditory PREDICTIVE and REACTIVE tasks cannot be explained by differences in saccade metrics.

Imaging

We conducted two contrasts subtracting auditory from visual blocks for both PREDICTIVE and REACTIVE tasks (Figure 7). As expected, when comparing auditory with visual conditions, we found greater activation in auditory cortex (bilateral superior temporal gyrus) for the auditory tasks and greater activation in visual cortex (bilateral middle occipital gyrus) for the visual tasks (Figure 7).

Tables 3 and 4 list the locations in Talairach coordinates of the main peaks of activation clusters for the contrasts of interest. We first contrasted brain activation patterns between the PREDICTIVE and REACTIVE tasks with visual and auditory conditions collapsed. Results from this contrast revealed a similar network of brain areas that were activated for PREDICTIVE and REACTIVE tasks (Figure 8). For the PREDICTIVE task (warm colors),

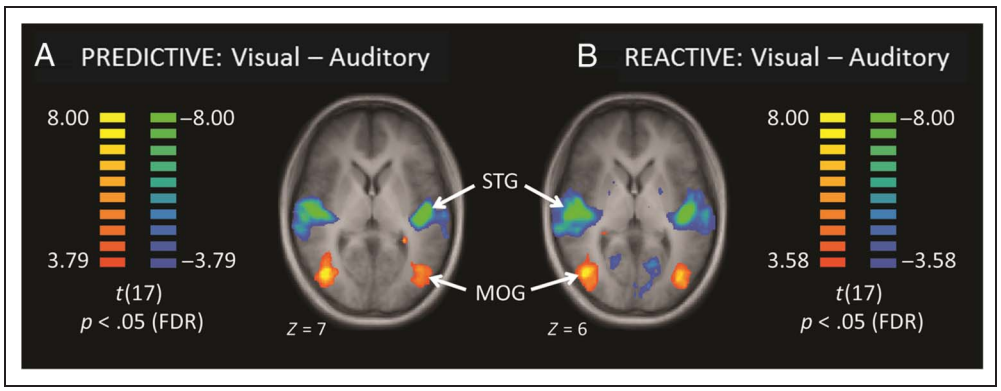

Figure 7. Experiment 3. Contrast maps subtracting auditory from visual blocks for the (A) predictive saccade task and (B) reactive saccade task. Images were thresholded at $p < .05$ (FDR-corrected) and at cluster sizes of at least 9 voxels. STG = superior temporal gyrus; MOG = middle occipital gyrus.

Table 3. Experiment 3: MRI Activation Peaks for PREDICTIVE–REACTIVE (Visual)

	Talairach Coordinates				
Anatomical Region	*x*	*y*	*z*	*t*	*Size (Voxels)*
PREDICTIVE > REACTIVE					
mPFC	−12	47	13	7.56	292
L insula (posterior)	−45	−13	22	7.35	28
L IFG	−39	29	10	5.85	44
L PCC	−21	−52	16	5.99	112
R PCC	21	−58	16	5.88	44
L paracentral lobule	−3	−25	46	5.55	21
L parahippocampal gyrus	−27	−7	−11	6.24	91
R parahippocampal gyrus	27	−37	−2	5.89	75
L STG	−36	−52	22	5.20	14
R cuneus	6	−85	22	6.63	278
L caudate	−6	8	4	5.55	21
R cerebellum (crus I)	21	−73	−35	5.18	31
REACTIVE > PREDICTIVE					
SEF	3	−1	61	7.90	183
R FEF	21	−7	52	6.98	154
L FEF	−24	−7	46	6.52	110
R STG	51	−37	19	5.78	32
R MTG	48	−67	7	5.03	30
R cerebellum (lobule VI)	33	−46	−20	5.19	17

x, *y*, *z* Talairach coordinates specify the location of the peak voxel (highest *t* value) of a cluster in an anatomical region. L = left, R = right; IFG, inferior frontal gyrus; STG/MTG, superior and middle temporal gyrus.

we observed greater activation in the mPFC, PCC, IPL, bilateral hippocampus, and the cerebellum (crus I). We again observed greater activation in the oculomotor brain areas including the right DLPFC, SEF, bilateral FEF, PEF, and cerebellum (lobule VI) for the REACTIVE task (cool colors).

We also compared PREDICTIVE with REACTIVE within sensory modalities (i.e., visual, auditory; Figure 9). For the visual conditions (Figure 9A), the PREDICTIVE > REACTIVE contrast showed greater activation in areas including the mPFC, PCC, bilateral hippocampus, and cerebellum (crus I), whereas the REACTIVE > PREDICTIVE contrast revealed greater activation in areas including the SEF, FEF, and the cerebellum (lobule VI; see Table 3). For the auditory conditions (Figure 9B), we saw similar areas of activation for the equivalent contrasts (see Table 4). The PREDICTIVE > REACTIVE contrast again showed greater activation in areas including mPFC, PCC, bilateral hippocampus, and bilateral cerebellum (crus I). The REACTIVE > PREDICTIVE contrast revealed greater activation in the FEF, SEF, PEF, right DLPFC, and cerebellum (lobule VI). These results suggest that neural processing of the PREDICTIVE and REACTIVE tasks were similar between visual and auditory conditions.

Lastly, we conducted PREDICTIVE–REACTIVE for both the visual and auditory tasks (auditory contrast map not shown). In this contrast, we found no areas of activation that survived whole-brain correction (FDR, $p < .05$). This suggests that the brain activation patterns associated with PREDICTIVE–REACTIVE were similar between visual and auditory conditions.

DISCUSSION

We investigated the neural mechanisms underlying prediction and synchronization of eye movements by comparing the brain regions activated in a predictive

Table 4. Experiment 3: MRI Activation Peaks for PREDICTIVE–REACTIVE (Auditory)

	Talairach Coordinates				
Anatomical Region	*x*	*y*	*z*	*t*	*Size (Voxels)*
PREDICTIVE > REACTIVE					
L SFG	−21	17	40	7.88	407
L pFC	−36	41	−2	7.11	559
R pFC	39	38	−5	5.12	26
L ACC/ventral mPFC	−18	56	19	5.68	34
R ACC/ventral mPFC	3	14	−2	6.94	222
L dorsal mPFC	−6	53	37	6.52	496
R dorsal mPFC	3	65	25	6.34	139
L MFG	−45	23	22	6.16	100
L paracentral lobule	−9	−34	64	5.28	12
R paracentral lobule	9	−31	61	6.47	160
L insula (posterior)	−36	−13	16	7.59	76
R insula (posterior)	33	−13	22	8.16	115
Cingulate gyrus	0	38	−2	5.39	108
L PCC	−15	62	10	6.39	849
R PCC	6	−55	25	5.83	35
L IPL	−36	−61	28	6.37	345
R IPL	39	−64	25	5.59	109
L precuneus	−3	−67	28	5.33	43
R postcentral gyrus	24	−31	61	4.16	83
L parahippocampal gyrus	−21	−28	−5	9.09	530
R parahippocampal gyrus	12	−37	7	8.34	550
L temporal pole	−45	8	−20	7.38	312
R temporal pole	42	17	−17	6.05	192
L MTG	−51	−40	−5	6.03	153
R MTG	57	−1	−14	5.41	65
L ITG	−57	−16	−14	3.84	20
R ITG	51	−61	−14	5.40	41
L lingual gyrus	−6	−88	−14	6.84	49
L MOG	−24	−91	19	5.83	93
R MOG	33	−82	16	5.33	163
L cuneus	−3	−91	31	5.36	145
R cuneus	18	−88	37	5.44	47
L cerebellum (crus I)	−33	−67	−32	5.87	89
R cerebellum (crus I)	27	−67	−35	5.54	308
R cerebellum (lobule X)	3	−43	−38	4.66	15

Table 4. (*continued*)

Anatomical Region	Talairach Coordinates			*t*	Size (Voxels)
	x	*y*	*z*		
REACTIVE > PREDICTIVE					
SEF	0	−1	55	10.53	1174
L FEF	−42	−7	46	9.74	264
R FEF	18	−10	52	9.03	171
L insula (anterior)	−27	17	10	6.24	17
R insula (anterior)	39	8	10	5.69	85
R DLPFC	22	38	22	5.38	60
L PEF	−27	−49	55	5.50	119
R PEF	6	−46	49	7.40	157
L STG	−54	−43	22	7.17	269
R STG	51	−37	19	11.02	491
L putamen	−18	−1	13	7.84	249
R putamen	21	−4	16	10.00	331
L thalamus	−15	−13	7	5.47	34
R thalamus	12	−13	13	7.08	22
L cerebellum (lobule VI)	−33	−52	−23	7.75	237
R cerebellum (lobule VI)	24	−40	−23	8.41	107
R cerebellum (declive)	0	−64	−17	6.56	105
R red nucleus	6	−19	−2	5.43	44

x, *y*, *z* Talairach coordinates specify the location of the peak voxel (highest *t* value) of a cluster in an anatomical region. L = left, R = right; SFG/MFG, superior and middle frontal gyrus; MTG/ITG, middle and inferior temporal gyrus; MOG, middle occipital gyrus; STG, superior temporal gyrus.

saccade task with those activated in a reactive saccade task. Regardless of the modality of sensory stimuli (visual or auditory), we consistently found increased activation in default network areas (mPFC, IPL, PCC, and hippocampus) and cerebellum crus I for PREDICTIVE and increased activation in oculomotor network areas (FEF, SEF, PEF, and DLPFC) and cerebellum lobule VI for REACTIVE. From our results, we make three important conclusions. First, the REACTIVE tasks recruited oculomotor areas to guide more complex responses. Second, activation of areas in the default network in the PREDICTIVE tasks suggested that participants were able to disengage from focusing on the task, which indicated that predictive saccades were easy, well-learned motor responses that required little mental effort. Finally, we dissociated two areas of the cerebellum (crus I vs. lobule VI) that appear to play different roles in the predictive control of saccades. This study clearly demonstrates that regardless of modality, there is a pronounced dissociation between REACTIVE and PREDICTIVE neural correlates, which is discussed in detail below.

REACTIVE and PREDICTIVE Saccades Compared with Fixation

Our initial contrast images produced comparing REACTIVE and PREDICTIVE to fixation suggested that behavior in these tasks differed in their dependency on oculomotor brain regions. Contrary to what previous saccade studies in patients have suggested (Pierrot-Deseilligny et al., 2004), our results clearly showed that predictive saccades following a simple rhythmic pattern appear to rely minimally on activation of cortical oculomotor regions. In fact, our results showed more prominent activation in these areas for the REACTIVE task, when target timing was not predictable. We did, however, observe a small cluster of activation more inferiorly in the lateral FEF for PREDICTIVE compared with fixation (Figure 4). Previous studies have shown different activations in the superior and inferior precentral sulcus in saccade tasks with differing cognitive load: More superior regions are associated with increased load (Merriam et al., 2001; Culham et al., 1998; Petit, Clark, Ingeholm, & Haxby, 1997). Therefore, the pattern of

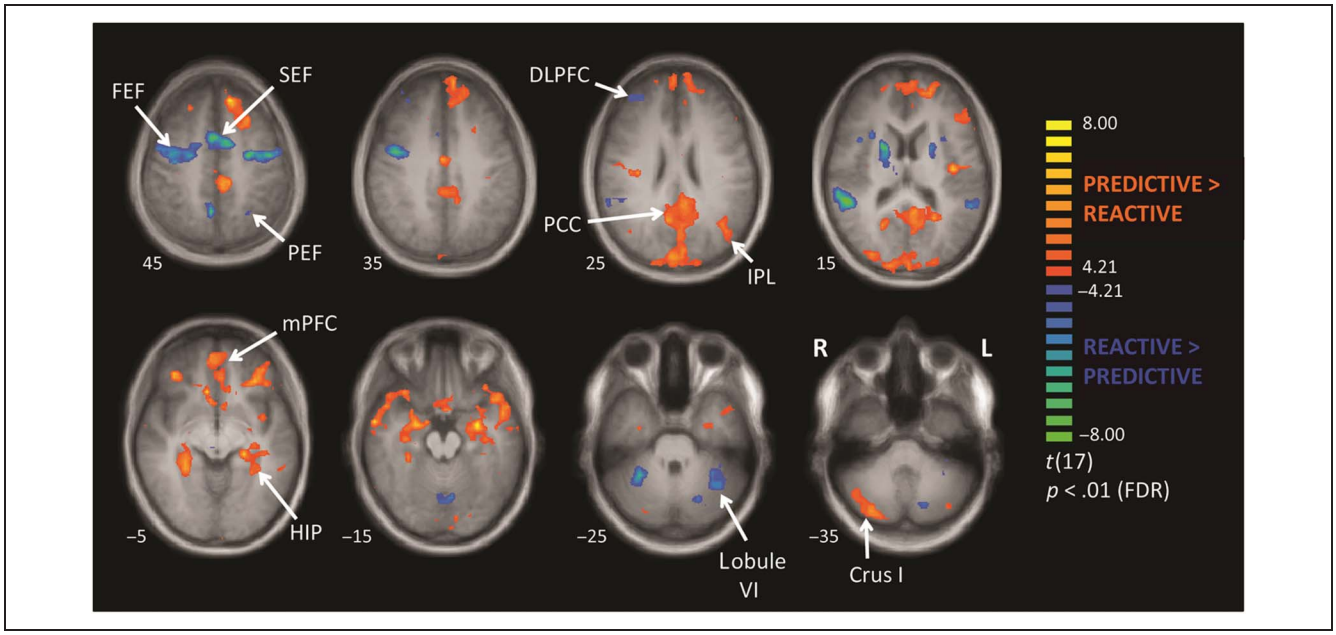

Figure 8. Experiment 3. Contrast map comparing the subtractions of saccade tasks with fixation. Auditory and visual conditions were collapsed. Voxels that yield positive values (PREDICTIVE > REACTIVE) are shown in orange/yellow and those that yield negative values (REACTIVE > PREDICTIVE) are shown in blue. Images were thresholded at $p < .01$ (FDR-corrected) and at cluster sizes of at least 9 voxels. Coordinates are in the Talairach z plane.

activation observed in PREDICTIVE > fixation may be because the PREDICTIVE task was simpler and imposed a lesser cognitive load than the REACTIVE task. This is not surprising because our REACTIVE task was essentially a more difficult timing task relative to the PREDICTIVE task.

Reactive Saccades Recruit the Oculomotor Network

From our results, it was not surprising that, compared with PREDICTIVE tasks, we observed greater activation in oculomotor areas (FEF, SEF, PEF and DLPFC) for REACTIVE tasks. These areas are well known to be involved within a larger oculomotor network (Müri, 2006) and from our functional connectivity analyses, we confirmed this by demonstrating significantly correlated activity between these four regions (Figure 5B). Contrary to our results, however, previous studies have implicated the role of the FEF, SEF and DLPFC in predictive saccades (Nyffeler et al., 2008; Pierrot-Deseilligny et al., 2004). The involvement of FEF and DLPFC was based on human lesion studies (Pierrot Deseilligny et al., 2003; Rivaud et al., 1994), whereas the role of SEF was revealed when predictive saccade deficits were observed after TMS (Nyffeler et al., 2008). Although we did not find activation in these areas during the PREDICTIVE task, this does not imply that they played no role for predictive saccades. Our results simply showed that behavior in the predictive task relies less on activation of frontal oculomotor areas relative to reactive saccades when timing was unpredictable.

Interestingly, our results follow closely with previous fMRI studies comparing regular and irregular finger tapping (Lutz et al., 2000) or predictive and reactive saccades (Simó et al., 2005). As mentioned earlier, we may be observing this activation pattern in the oculomotor network because of increased timing complexity in the REACTIVE task. Previous studies have found similar results with finger tapping tasks. For example, Dhamala et al. (2003) had participants perform rhythmic tapping while manipulating the number of beats to increase complexity. Similar to our results, they found activation correlated with complexity in primary motor cortex, SMA, BG, thalamus, and cerebellum. Another study also manipulated the complexity of an auditory rhythm in a sensorimotor synchronization task and found increased activation in bilateral SMA, premotor cortex, right DLPFC, and right primary motor cortex with increasing complexity (Lewis, Wing, Pope, Praamstra, & Miall, 2004). The authors argued that the DLPFC may be involved with error monitoring and correction. This is supported by another study that found increased DLPFC activation when participants tapped to increasingly modulated tone sequences compared with rhythmic isochronous tapping (Stephan et al., 2002). Therefore, it is possible in our study that oculomotor areas were recruited for the REACTIVE conditions to guide responses associated with greater timing complexity relative to the PREDICTIVE task.

Predictive Saccades Recruit the Default Network

Our results showed greater activation in the mPFC, PCC, IPL, and hippocampus for PREDICTIVE tasks compared with REACTIVE tasks. Simó et al. (2005) also found similar areas active in their equivalent contrast, including the IPL

and hippocampus. Our functional connectivity analyses revealed significantly correlated activity between all four of these areas (Figure 5A). Interestingly, there exists a rich literature showing these areas involved with a "default network," which has been demonstrated to be preferentially active when participants are not focused on their external environment (Mason et al., 2007; Mazoyer et al., 2001; Raichle et al., 2001; Shulman et al., 1997). These brain areas are associated with stimulus-independent thoughts, which are thoughts unrelated to the task. For example, greater activation in default network areas has been observed when rest was compared with an auditory attention task (Binder et al., 1999). When probed periodically, participants reported almost six times as many stimulus-independent thoughts during those rest periods than for the task. Other studies have manipulated task difficulty and found that easier tasks produced more of these thoughts than difficult tasks and that greater activation in the default network was associated with greater occurrences of stimulus-independent thoughts (McKiernan, D'Angelo, Kaufman, & Binder, 2006; McKiernan, Kaufman, Kucera-Thompson, & Binder, 2003). Similarly, in our study, the PREDICTIVE task was very simple, and saccades only alternated between two targets. The low cognitive demand of the task may have facilitated the participants' ability to perform the task with rhythmicity, leaving them in a mental state similar to that at rest. Therefore, participants engaging in task-unrelated thinking during the PREDICTIVE tasks may perhaps explain the observed activation in the default network. This is consistent with the notion that the REACTIVE task is a more difficult timing task compared with the PREDICTIVE task as mentioned earlier. These results, however, do not explain what is controlling the rhythmicity of predictive saccades. We propose that this responsibility lies predominantly with the cerebellum.

The Role of the Cerebellum in Timing

We consistently found activation in the cerebellum in both PREDICTIVE and REACTIVE tasks, which is not unexpected because its role in timing has been studied extensively (see Buhusi & Meck, 2005, for a review). For example, studies have demonstrated its involvement in movement timing (Penhune et al., 1998; Ivry, 1997; Ivry, Keele, & Diener, 1988), temporal prediction (Tesche & Karhu, 2000) and auditory rhythm processing (Thaut, 2009; Ivry, 2002; Schubotz, Friederici, & von Cramon, 2000; Griffiths, 1999; Sakai, 1999; Penhune et al., 1998). However, there has been less attention on functional dissociation within the

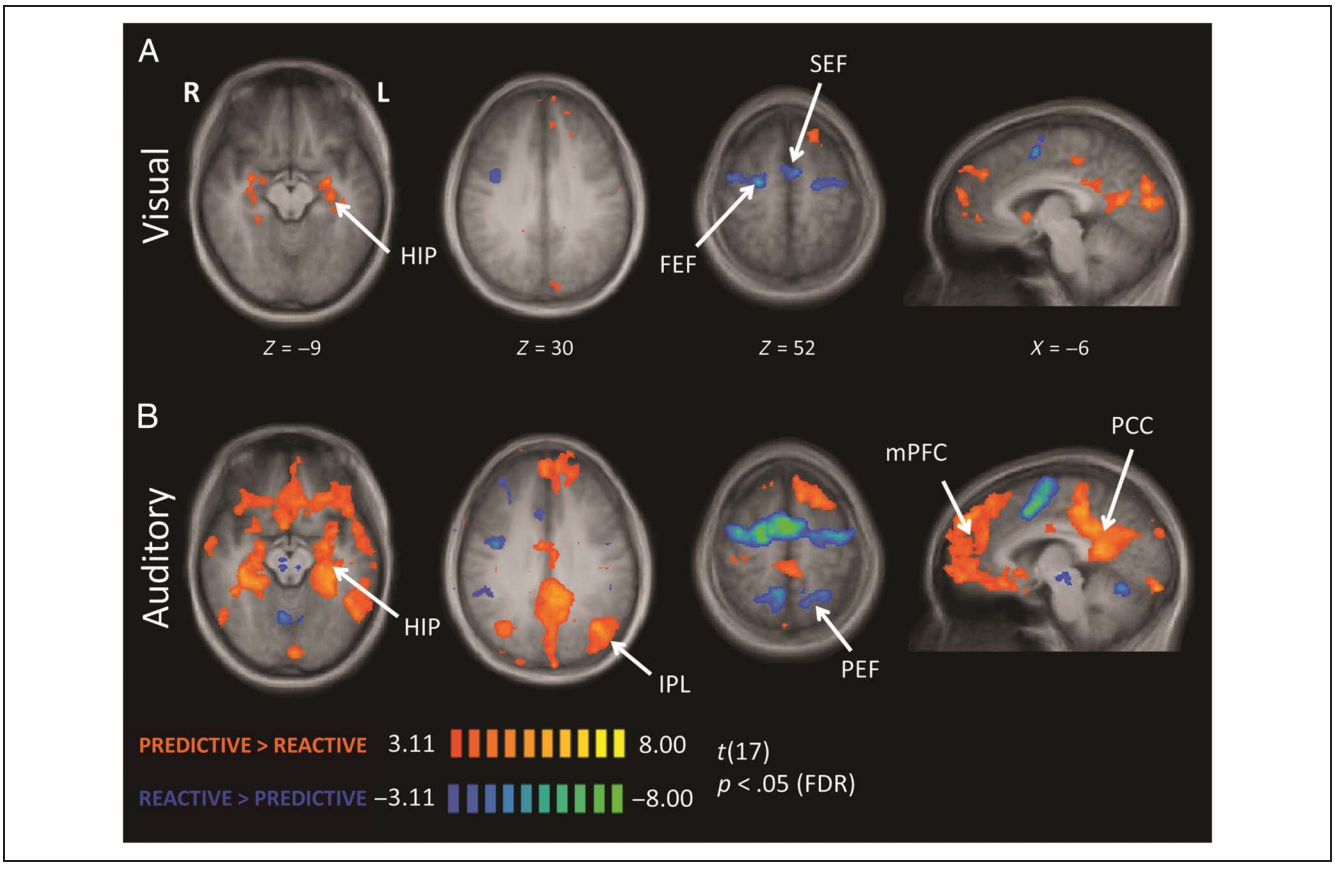

Figure 9. Experiment 3. Contrast maps displaying PREDICTIVE–REACTIVE for auditory (A) and visual (B) blocks. Voxels that yield positive values (PREDICTIVE > REACTIVE) are shown in orange/yellow, and those that yield negative values (REACTIVE > PREDICTIVE) are shown in blue/green. Images were thresholded at $p < .05$ (FDR-corrected) and at cluster sizes of at least 9 voxels.

cerebellum. In our results, we dissociated two significant areas of the cerebellum that appear to play different roles: lobule VI for reactive saccades and crus I for predictive saccades.

Many studies have observed increased activation in lobule VI when comparing random to regular motor responses (Simó et al., 2005; Lutz et al., 2000). This region of the cerebellum appears to be involved with processing more complex temporal patterns, such as random sequences. For example, Dhamala et al. (2003) found lobule VI activation associated with finger tapping to increasingly complex rhythms. In addition to a random sequence, Stephan et al. (2002) modulated a tapping sequence at three different levels and compared the behavior to isochronous tapping. They found that increased modulation and random sequences were both associated with increased activation in lobule VI. These observations together with the results from our study suggest that cerebellar lobule VI is responsible for processing more complex and irregular temporal patterns. This is unsurprising given that this paradigm relies on predictive timing only, placing visual targets at known locations paced at regular intervals. A critical next step is to manipulate spatial prediction, both with and without temporal prediction to differentiate timing relative to other components of prediction.

Posterior to lobule VI is the cerebellar crus I, which we found consistently activated during PREDICTIVE tasks. A previous fMRI study comparing predictive saccades with reactive saccades also found activation in this area (Simó et al., 2005). The same was observed when tapping to regular sequences was compared with irregular (Lutz et al., 2000). Period and phase correction are important processes that enable the performance of accurate and synchronous motor responses to an external rhythm, and Lutz et al. (2000) suggested that this cerebellar region, crus I, may be particularly important for phase correction during sensorimotor synchronization. However, this seems unlikely because patients with cerebellar lesions perform as well as healthy controls in their ability to adapt to perturbations to a metronome sequence (Molinari, 2003), as well as their ability to learn an auditory rhythm to guide tapping responses (Molinari et al., 2005). A more recent study has suggested that crus I may in fact be important in working memory (Konoike, 2012). More specifically, it is preferentially activated during encoding and retrieval processes underlying regular synchronous tapping. It is possible that crus I activation in our results reflect a similar working memory process guiding sensorimotor synchronized movements in the form of predictive saccades.

However, we know from transneuronal staining techniques in nonhuman primates that crus I possesses both efferent and afferent projections to the pFC (Kelly & Strick, 2003; Middleton & Strick, 1994, 2001). Furthermore, recent functional connectivity work has revealed correlations between crus I and the mPFC during resting state MRI (Buckner, Krienen, Castellanos, Diaz, & Yeo, 2011; Krienen & Buckner, 2009), implicating crus I involvement in the default network. Therefore, it is more likely that we observed crus I recruitment because of the cognitive simplicity of the task (e.g., defaulting into resting state) rather than an underlying mechanism for prediction itself. Interestingly, Krienen and Buckner (2009) also noted that lobule VI is correlated with the anterior pFC, which is consistent with the lack of overlap we observed in cerebellar recruitment between predictive and reactive conditions.

Summary and Conclusions

The neural control of sensorimotor synchronization with saccades is similar to that of isochronous finger tapping. We provide parsimonious explanations for the discrepancies in the saccade literature between recent neuroimaging studies (Simó et al., 2005; O'Driscoll et al., 2000) with evidence from lesion studies for the predictive saccade task (Nyffeler et al., 2008; Pierrot Deseilligny et al., 2003; Rivaud et al., 1994). We provide evidence for two separate brain networks preferentially recruited during a simple predictive and a more difficult reactive saccade task. The reactive task revealed activation in oculomotor network areas reflecting the increased level of complexity of the timing task, whereas the predictive task revealed activation in the default network reflecting the low cognitive demand of the task. Finally, we revealed an important functional dissociation within the cerebellum: crus I activation is associated with predictive saccades, likely via the default network, and lobule VI activation is associated with reactive saccades. Future studies may be directed toward further characterizing the role of crus I in sensorimotor synchronization.

Acknowledgments

Special thanks to all Munoz Lab members for their editorial assistance and Sharon David for MRI technical support. This work was supported by a research operating grant from the Canadian Institute of Health Research (MOP-97741) and the Ontario Research Fund to D. P. M.

Reprint requests should be sent to Douglas P. Munoz, Centre for Neuroscience Studies, 18 Stuart St., Kingston, ON, Canada K7L 2N8, or via e-mail: doug.munoz@queensu.ca.

REFERENCES

Amaro, E., Jr., & Barker, G. J. (2006). Study design in fMRI: Basic principles. *Brain and Cognition, 60,* 220–232.

Bijsterbosch, J. D., Lee, K., Hunter, M. D., Tsoi, D. T., Lankappa, S., Wilkinson, I. D., et al. (2011). The role of the cerebellum in sub- and supraliminal error correction during sensorimotor synchronization: Evidence from fMRI and TMS. *Journal of Cognitive Neuroscience, 23,* 1100–1112.

Binder, J. R., Frost, J. A., Hammeke, T. A., Bellgowan, P. S. F., Rao, S. M., & Cox, R. W. (1999). Conceptual processing

during the conscious resting state: A functional MRI study. *Journal of Cognitive Neuroscience, 11,* 80–93.
Buckner, R. L., Krienen, F. M., Castellanos, A., Diaz, J. C., & Yeo, B. T. (2011). The organization of the human cerebellum estimated by intrinsic functional connectivity. *Journal of Neurophysiology, 106,* 2322–2345.
Buhusi, C. V., & Meck, W. H. (2005). What makes us tick? Functional and neural mechanisms of interval timing. *Nature Reviews. Neuroscience, 6,* 755–765.
Chen, J. L., Penhune, V. B., & Zatorre, R. J. (2008). Listening to musical rhythms recruits motor regions of the brain. *Cerebral Cortex, 18,* 2844–2854.
Chen, J. L., Zatorre, R. J., & Penhune, V. B. (2006). Interactions between auditory and dorsal premotor cortex during synchronization to musical rhythms. *Neuroimage, 32,* 1771–1781.
Culham, J. C., Brandt, S. A., Cavanagh, P., Kanwisher, N. G., Dale, A. M., & Tootell, R. B. H. (1998). Cortical fMRI activation produced by attentive tracking of moving targets. *Journal of Neurophysiology, 80,* 2657–2670.
Dhamala, M., Pagnoni, G., Wiesenfeld, K., Zink, C. F., Martin, M., & Berns, G. S., (2003). Neural correlates of the complexity of rhythmic finger tapping. *Neuroimage, 20,* 918–926.
Fischer, B., Biscaldi, M., & Gezeck, S. (1997). On the development of voluntary and reflexive components in human saccade generation. *Brain Research, 754,* 285–297.
Gerloff, C., Richard, J., Hadley, J., Schulman, A. E., Honda, M., & Hallett, M. (1998). Functional coupling and regional activation of human cortical motor areas during simple, internally paced and externally paced finger movements. *Brain, 121,* 1513–1531.
Griffiths, T. D. (1999). A common neural substrate for the analysis of pitch and duration pattern in segmented sound? *NeuroReport, 10,* 3825.
Isotalo, E., Lasker, A. G., & Zee, D. S. (2005). Cognitive influences on predictive saccadic tracking. *Experimental Brain Research, 165,* 461–469.
Ivry, R. B. (1997). Cerebellar timing systems. *International Review of Neurobiology, 41,* 555–573.
Ivry, R. B. (2002). The cerebellum and event timing. *Annals of the New York Academy of Sciences, 978,* 302–317.
Ivry, R. B., Keele, S., & Diener, H. (1988). Dissociation of the lateral and medial cerebellum in movement timing and movement execution. *Experimental Brain Research, 73,* 167–180.
Ivry, R. B., & Spencer, R. M. (2004). The neural representation of time. *Current Opinion in Neurobiology, 14,* 225–232.
Jäncke, L., Loose, R., Lutz, K., Specht, K., & Shah, N. J. (2000). Cortical activations during paced finger-tapping applying visual and auditory pacing stimuli. *Cognitive Brain Research, 10,* 51–66.
Joiner, W. M., & Shelhamer, M. (2006). An internal clock generates repetitive predictive saccades. *Experimental Brain Research, 175,* 305–320.
Kelly, R. M., & Strick, P. L. (2003). Cerebellar loops with motor cortex and prefrontal cortex of a nonhuman primate. *Journal of Neuroscience, 23,* 8432–8444.
Knyazeva, M. G., Kurganskaya, M. E., Kurgansky, A. V., Njiokiktjien, C. J., & Vildavsky, V. J. (1994). Interhemispheric interaction in children of 7–8: Analysis of EEG coherence and finger tapping parameters. *Behavioural Brain Research, 61,* 47–58.
Kolers, P. A., & Brewster, J. M. (1985). Rhythms and responses. *Journal of Experimental Psychology: Human Perception and Performance, 11,* 150–167.
Konoike, N. N. (2012). Rhythm information represented in the fronto-parieto-cerebellar motor system. *Neuroimage, 63,* 328–338.
Krienen, F. M., & Buckner, R. L. (2009). Segregated front-cerebellar circuits revealed by intrinsic functional connectivity. *Cerebral Cortex, 19,* 2485–2497.
Kwong, K. K., Belliveau, J. W., Chesler, D. A., Goldberg, I. E., Weisskoff, R. M., Poncelet, B. P., et al. (1992). Dynamic magnetic resonance imaging of human brain activity during primary sensory stimulation. *Proceedings of the National Academy of Sciences, U.S.A., 89,* 5675–5679.
Lewis, P. A., Wing, A. M., Pope, P. A., Praamstra, P., & Miall, R. C. (2004). Brain activity correlates differentially with increasing temporal complexity of rhythms during initialisation, synchronisation, and continuation phases of paced finger tapping. *Neuropsychologia, 42,* 1301–1312.
Lutz, K., Specht, K., Shah, N. J., & Jancke, L. (2000). Tapping movements according to regular and irregular visual timing signals investigated with fMRI. *NeuroReport, 11,* 1301–1306.
Mason, M. F., Norton, M. I., Van Horn, J. D., Wegner, D. M., Grafton, S. T., & Macrae, C. N. (2007). Wandering minds: The default network and stimulus-independent thought. *Science, 315,* 393–395.
Mazoyer, B., Zago, L., Mellet, E., Bricogne, S., Etard, O., Houdé, O., et al. (2001). Cortical networks for working memory and executive functions sustain the conscious resting state in man. *Brain Research Bulletin, 54,* 287–298.
McKiernan, K. A., D'Angelo, B. R., Kaufman, J. N., & Binder, J. R. (2006). Interrupting the "stream of consciousness": An fMRI investigation. *Neuroimage, 29,* 1185–1191.
McKiernan, K. A., Kaufman, J. N., Kucera-Thompson, J., & Binder, J. R. (2003). A parametric manipulation of factors affecting task-induced deactivation in functional neuroimaging. *Journal of Cognitive Neuroscience, 15,* 394–408.
Merriam, E. P., Colby, C. L., Thulborn, K. R., Luna, B., Olson, C. R., & Sweeney, J. A. (2001). Stimulus–response incompatibility activates cortex proximate to three eye fields. *Neuroimage, 13,* 794–800.
Middleton, F. A., & Strick, P. L. (2001). Cerebellar projections to the prefrontal cortex of the primate. *Journal of Neuroscience, 21,* 700–712.
Middleton, F. A., & Strick, P. L. (1994). Anatomical evidence for cerebellar and basal ganglia involvement in higher cognitive function. *Science, 266,* 458–461.
Molinari, M., Leggio, M. G., Filippini, V., Gioia, M. C., Cerasa, A., & Thaut, M. H. (2005). Sensorimotor transduction of time information is preserved in subjects with cerebellar damage. *Brain Research Bulletin, 67,* 448–458.
Molinari, M. M. (2003). Neurobiology of rhythmic motor entrainment. *Annals of the New York Academy of Sciences, 999,* 313–321.
Munoz, D. P., Broughton, J. R., Goldring, J. E., & Armstrong, I. T. (1998). Age-related performance of human subjects on saccadic eye movement tasks. *Experimental Brain Research, 121,* 391–400.
Müri, R. M. (2006). MRI and fMRI analysis of oculomotor function. *Progress in Brain Research, 151,* 503–526.
Nyffeler, T., Rivaud-Pechouix, S., Wattiez, N., & Gaymard, B. (2008). Involvement of the supplementary eye field in oculomotor predictive behavior. *Journal of Cognitive Neuroscience, 20,* 1583–1594.
O'Driscoll, G. A., Wolff, A. V., Benkelfat, C., Florencio, P. S., Lal, S., & Evans, A. C. (2000). Functional neuroanatomy of smooth pursuit and predictive saccades. *NeuroReport, 11,* 1335–1340.

Ogawa, S., Lee, T. M., Kay, A. R., & Tank, D. W. (1990). Brain magnetic resonance imaging with contrast dependent on blood oxygenation. *Proceedings of the National Academy of Sciences, U.S.A., 87,* 9868–9872.

Peltsch, A., Hemraj, A., Garcia, A., & Munoz, D. P. (2011). Age-related trends in saccade characteristics among the elderly. *Neurobiology of Aging, 32,* 669–679.

Penhune, V. B., Zatorre, R. J., & Evans, A. C. (1998). Cerebellar contributions to motor timing: A PET study of auditory and visual rhythm reproduction. *Journal of Cognitive Neuroscience, 10,* 752–765.

Petit, L., Clark, V. P., Ingeholm, J., & Haxby, J. V. (1997). Dissociation of saccade-related and pursuit-related activation in human frontal eye fields as revealed by fMRI. *Journal of Neurophysiology, 77,* 3386–3390.

Pierrot-Deseilligny, C., Milea, D., & Müri, R. M. (2004). Eye movement control by the cerebral cortex. *Current Opinion in Neurology, 17,* 17–25.

Pierrot Deseilligny, C., Müri, R. M., Ploner, C. J., Gaymard, B., Demeret, S., & Rivaud Pechoux, S. (2003). Decisional role of the dorsolateral prefrontal cortex in ocular motor behaviour. *Brain, 126,* 1460–1473.

Pierrot-Deseilligny, C., Rivaud, S., Gaymard, B., & Agid, Y. (1991). Cortical control of reflexive visually guided saccades. *Brain, 114,* 1473–1485.

Pollok, B., Gross, J., Müller, K., Aschersleben, G., & Schnitzler, A. (2005). The cerebral oscillatory network associated with auditorily paced finger movements. *Neuroimage, 24,* 646–655.

Pollok, B., Krause, V., Butz, M., & Schnitzler, A. (2009). Modality specific functional interaction in sensorimotor synchronization. *Human Brain Mapping, 30,* 1783–1790.

Raichle, M. E., MacLeod, A. M., Snyder, A. Z., Powers, W. J., Gusnard, D. A., & Shulman, G. L. (2001). A default mode of brain function. *Proceedings of the National Academy of Sciences, U.S.A., 98,* 676–682.

Rao, S. M., Harrington, D. L., Haaland, K. Y., Bobholz, J. A., Cox, R. W., & Binder, J. R. (1997). Distributed neural systems underlying the timing of movements. *Journal of Neuroscience, 17,* 5528–5535.

Repp, B. H. (2005). Sensorimotor synchronization: A review of the tapping literature. *Psychonomic Bulletin & Review, 12,* 969–992.

Rivaud, S., Müri, R., Gaymard, B., Vermersch, A., & Pierrot-Deseilligny, C. (1994). Eye movement disorders after frontal eye field lesions in humans. *Experimental Brain Research, 102,* 110–120.

Roebroeck, A., Formisano, E., & Goebel, R. (2005). Mapping directed influence over the brain using Granger causality and fMRI. *Neuroimage, 25,* 230–242.

Sakai, K. (1999). Neural representation of a rhythm depends on its interval ratio. *Journal of Neuroscience, 19,* 10074.

Schmahmann, J. D., Doyon, J., McDonald, D., Holmes, C., Lavoie, K., Hurwitz, A. S., et al. (1999). Three-dimensional MRI atlas of the human cerebellum in proportional stereotaxic space. *Neuroimage, 10,* 233–260.

Schubotz, R. I., Friederici, A. D., & von Cramon, D. Y. (2000). Time perception and motor timing: A common cortical and subcortical basis revealed by fMRI. *Neuroimage, 11,* 1–12.

Shulman, G. L., Fiez, J. A., Corbetta, M., Buckner, R. L., Miezin, F. M., Raichle, M. E., et al. (1997). Common blood flow changes across visual tasks: II. Decreases in cerebral cortex. *Journal of Cognitive Neuroscience, 9,* 648–663.

Simó, L. S., Krisky, C. M., & Sweeney, J. A. (2005). Functional neuroanatomy of anticipatory behavior: Dissociation between sensory-driven and memory-driven systems. *Cerebral Cortex, 15,* 1982–1991.

Stark, L., Vossius, G., & Young, L. R. (1962). Predictive control of eye tracking movements. *IRE Transactions on Human Factors in Electronics, HFE-3,* 52–57.

Stephan, K. M., Thaut, M. H., Wunderlich, G., Schicks, W., Tian, B., Tellmann, L., et al. (2002). Conscious and subconscious sensorimotor synchronization—Prefrontal cortex and the influence of awareness. *Neuroimage, 15,* 345–352.

Svoboda, J., Sovka, P., & Stancák, A. (2002). Intra- and inter-hemispheric coupling of electroencephalographic 8–13 Hz rhythm in humans and force of static finger extension. *Neuroscience Letters, 334,* 191–195.

Talairach, J., & Tournoux, P. (1988). *Co-planar stereotaxic atlas of the human brain*. Stuttgart: Thieme.

Tesche, C. D., & Karhu, J. J. T. (2000). Anticipatory cerebellar responses during somatosensory omission in man. *Human Brain Mapping, 9,* 119–142.

Thaut, M. M. H. (2009). Distinct cortico-cerebellar activations in rhythmic auditory motor synchronization. *Cortex, 45,* 44–53.